Rheology of Side-Group Liquid-Crystalline Polymers: Effect of Isotropic–Nematic Transition and Evidence of Flow Alignment

Rangaramanujam M. Kannan and Julia A. Kornfield*

Chemical Engineering Department, California Institute of Technology, Pasadena, California 91125

Norbert Schwenk and Christine Boeffel

Max-Planck-Institut für Polymerforschung, W-6500 Mainz, Germany

Received November 16, 1992; Revised Manuscript Received January 7, 1993

ABSTRACT: The dynamics of a nematic side-group liquid-crystalline polymer (SG-LCP) melt are investigated using transient stress and birefringence measurements. This SG-LCP shows a pronounced drop in the dynamic moduli at sufficiently low frequency upon passing through the transition from the isotropic to the nematic state. In contrast to previous studies, this suggests that liquid-crystalline order does affect the relaxation dynamics of SG-LCP melts. In the isotropic phase we simultaneously measure dynamic birefringence and stress to determine the stress-optic ratio (SOR). Results in the isotropic state near T_{ni} show the anomalously large SOR characteristic of pretransitional effects in liquid-crystalline systems in general. In the nematic state, we find that prolonged, large-amplitude oscillatory shear dramatically reduces the turbidity and increases the birefringence of the sample, suggesting that shearing induces a preferred alignment in this SG-LCP melt. This is accompanied by a decrease in the effective dynamic moduli of the nematic.

1. Introduction

Side-group liquid-crystalline polymers (SG-LCP) consist of a flexible polymeric backbone with mesogenic units attached to it as side groups (Figure 1a). The combination of anisotropic phase structure, capacity to freeze liquid-crystalline order into the glassy state, and ability to manipulate the orientation of their optical axis using applied fields makes SG-LCPs attractive for a variety of potential commercial applications, including optical data storage media, nonlinear optical materials, and stress sensors.[1] To realize these applications, it is imperative to understand the rheology of these materials and the effect of flow history on molecular alignment, which controls their optical and mechanical properties. Although considerable work has been done on main-chain and rigid-rod polymer liquid crystals, relatively little research has been devoted to the rheological behavior of SG-LCPs.

The few studies of SG-LCP melt rheology that have been reported[2-4] conclude that the flexible backbone dominates the rheology of nematic SG-LCPs, suppressing any significant manifestation of their liquid-crystalline character. This is rather surprising, given the profound effect of liquid-crystalline order on the rheology of small-molecule LCs,[5] thermotropic main-chain LCPs,[6] and lyotropic rodlike LCPs.[7,8] The fluid dynamics of SG-LCP melts are expected to be more complex than initial studies suggest, because they depend not only on the polymeric nature of the backbone but also on the liquid-crystalline nature of the mesogen and the coupling between the backbone and mesogen dynamics. Therefore, it is important to determine the role of liquid crystallinity in SG-LCP rheology and the origin of the qualitative distinctions between SG-LCPs and other types of liquid crystals.

Further, like ordered block-copolymer (BCPs) melts, SG-LCPs belong to a class of polymeric liquids that have intrinsically anisotropic microstructure and properties. This general characteristic is believed to be responsible for the flow-induced alignment observed in BCPs.[9] On this basis, one would expect flow alignment to occur in SG-LCPs as well. Earlier studies suggested that the liquid-crystalline character does not affect the viscoelastic properties of SG-LCPs.[2-4] Therefore, it has been inferred that they cannot be aligned using flow.[2] Our results show this conclusion to be premature and suggest that there are numerous analogies between the rheology of SG-LCPs and BCPs.

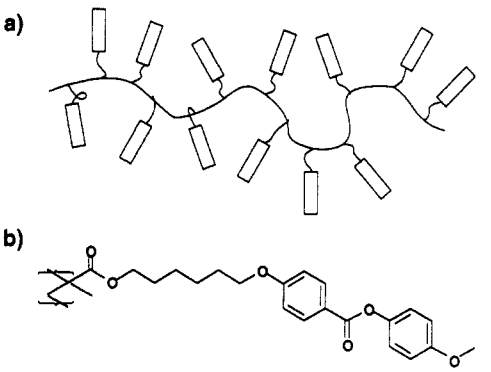

Figure 1. (a) Schematic diagram of a side-group liquid-crystalline polymer (SG-LCP). (b) The SG-LCP used in this study consists of a methacrylate backbone, a hexamethylene spacer, and a phenyl benzoate mesogen with a methoxy terminal group. Phase transitions: g 317 K (44 °C) n 390 K (117 °C) i.

After briefly reviewing the previous experimental and theoretical results that motivate us to examine the rheological and stress-optical behavior of SG-LCP melts, we describe the particular polymer we have chosen as a model system and the instrument and methods we use. Then we present results of dynamic stress and birefringence measurements, followed by our conclusions regarding the effects of both the isotropic–nematic transition and flow history in the nematic phase on the viscoelastic and optical properties of this SG-LCP melt.

2. Background

The isotropic-to-nematic transition generally produces a decrease in the viscosity of a liquid crystal. This is true for low molecular weight thermotropic LCs,[5] thermotropic main-chain LCPs,[6] and lyotropic rigid-rod LCPs.[7,8] This general trend can be understood by considering the relatively simple case of solutions of rigid-rod polymers. The physical picture captured by the Doi theory of

0024-9297/93/2226-2050$04.00/0

lyotropic rigid-rod LCPs is that the motion of a particular rod in an isotropic phase is severely hindered by the "cage" of neighboring, isotropically oriented rods; in the nematic phase, the tendency of the rods to align with one another produces a dilation of this "cage" and increases the rotational diffusivity.[10] At the isotropic–nematic transition, this accelerates relaxation dynamics and consequently reduces the viscosity. The general applicability of this qualitative picture is consistent with the observation that the viscosity decreases upon transition from the isotropic to the nematic state for both thermotropic and lyotropic systems for polymeric and low molecular weight liquid crystals.

Therefore, the presence of liquid-crystalline order is expected to play a significant role in determining the viscoelastic properties of SG-LCP melts as well. Indeed, this is evident in the decrease in the modulus at the isotropic-to-nematic transition of SG-LCP networks.[11] Surprisingly, however, corresponding effects have not been found in the previous studies of SG-LCP melts. Low shear rate viscosity measurements by Fabre and Veyssie[2] on SG-LCPs showed the viscosity to be a continuous function of temperature, with no drop at the isotropic–nematic transition. This led them to believe that the dynamic viscoelastic behavior in the nematic state is dominated by the polymeric backbone. Similarly, Zentel and Wu[3] studied various SG-LCPs with polymethacrylate, polyacrylate, and poly(chloroacrylate) main-chain and phenyl benzoate side groups with different spacer lengths and terminal groups and found that the low-shear viscosity increases monotonically with decreasing temperature even at T_{ni}. From this, they concluded that ordering does *not* affect the viscoelastic properties and, therefore, inferred that shear cannot be effective in inducing alignment in the sample. A recent study of the dynamic moduli of SG-LCP melts also revealed no effect of the isotropic–nematic phase transition on the relaxation dynamics of the melt.[4] However, there is evidence that, in LCPs with mesogens in both the main chain and the side chains, liquid crystallinity *does* affect the dynamics. Pakula and Zentel[12] found that the isotropic–nematic transition of such a polymer is accompanied by a significant decrease in the dynamic moduli in oscillatory shear at a fixed frequency. The origin of these apparently contradictory results is not yet understood.

Other manifestations of liquid-crystalline nature are the pretransitional phenomena that are predicted by the Landau–de Gennes theory of thermotropic LCs[13,14] and the Doi theory for lyotropic rigid-rod LCs.[10] These phenomena arise because the closer the system is to the isotropic–nematic transition, where it will spontaneously align, the smaller the driving force required to produce a given degree of molecular orientation. This is characterized by an increase in the ratio of birefringence to the strength of an applied field. In low molecular weight liquid crystals, this effect is readily observed in their response to magnetic or electric fields;[15,16] in SG-LCPs, pretransitional phenomena are more pronounced in response to stress fields.[17-19] This distinction may arise because accessible magnetic or electric torques can rapidly align the mesogens of a small-molecule liquid crystal due to their low viscosity. These torques realign mesogens only very slowly in the much more viscous side-group liquid-crystalline polymers. However, high values of stress are easily achieved; therefore, rheooptical methods provide appropriate means to study pretransitional effects in LCPs. The ratio of birefringence to stress (the stress-optic ratio) has been found to increase strongly with approach to the isotropic–nematic transition of lyotropic rodlike LCPs[20] and of SG-LCP elastomers.[18] Here we characterize the behavior of the stress-optic ratio as a function of temperature and shear frequency in the isotropic phase of the present SG-LCP.

To clarify the manifestation of the liquid-crystalline nature of nematic SG-LCPs in their rheological properties, we apply dynamic viscoelastic measurements that have proven to be sensitive to phase transitions and alignment in other ordering systems, particularly block copolymers.[21] For example, in block-copolymer melts the viscoelastic response at high enough frequencies arises only from local, intramolecular response and thus is essentially unchanged when the polymer melt passes through the order–disorder transition (ODT). At low frequencies, slower microstructural dynamics contribute to the viscoelastic behavior, and these can suffer a discontinuous jump at phase transitions, such as the sharp increase in the dynamic moduli of block-copolymer melts at the ODT. One of the questions we address is the possibility of similar behavior in SG-LCP melts, with the distinction that the low-frequency moduli would decrease upon "ordering", i.e., passing from the isotropic to the nematic state.

Technologically, understanding the microrheology of SG-LCPs may lead to an effective means to control molecular alignment using flow. The proposed applications of SG-LCPs[1] require a uniformly oriented initial state onto which information can be written by locally heating to the isotropic state. Upon subsequent cooling into the liquid-crystalline state in the absence of an aligning field, that local region becomes riddled with orientational defects and has no preferred orientation. This provides the optical contrast used for reading information. To commercialize such applications, one must produce uniformly aligned SG-LCPs. The established methods of aligning SG-LCPs are extensions of the procedures applied to small-molecule LCs. All of these involve prolonged annealing in the presence of an aligning force provided by a very strong electric field, magnetic field, or surface effect. Using high field strengths and long annealing times leads to high processing costs. Surface effects are limited to thin films ($\lesssim$10 μm). Thus, advances in controlling molecular orientation to prepare monodomain materials could significantly influence the range of viable applications.

The presence of the flexible chain backbone may provide an alternative means of alignment using macroscopic deformation. Recent results on SG-LCP networks suggest that a small extension of the elastomer (roughly 10%) provides a more powerful means of inducing alignment than the strongest available electric or magnetic field.[18,19] In addition, shear flow has been found to be very effective in macroscopically ordering diblock and triblock copolymer melts.[9] If this phenomenon is general to fluids that possess intrinsically anisotropic structure, it can be expected to occur in SG-LCPs as well. Together, these observations motivate experiments to determine the effect of flow on the alignment of SG-LCPs. Should mechanical forces be successful in orienting SG-LCP melts, flow-induced alignment will be an attractive alternative to the established methods, because it is relatively inexpensive and applicable to arbitrarily thick samples.

3. Experimental Section

3.1. Materials. The side-group liquid-crystalline polymer chosen for this research consists of a methacrylate backbone, a six-methylene spacer, and a phenyl benzoate mesogenic group (Figure 1b).[22] The terminal group on the mesogen is a methoxy moiety, which results in a material with a nematic phase over a

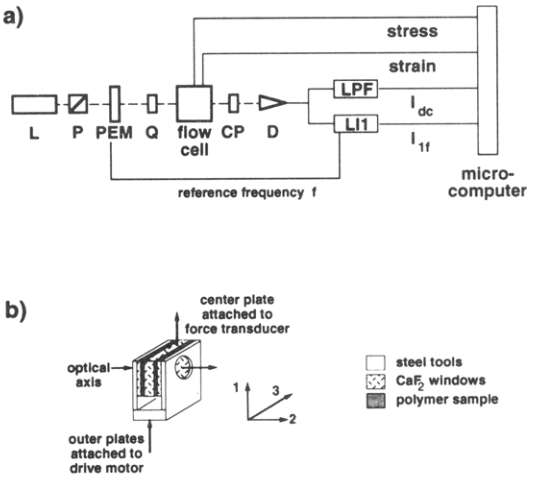

Figure 2. (a) Schematic diagram of the apparatus for simultaneous mechanical and optical measurements. Components of the optical train: laser L, linear polarizer P, photoelastic modulator PEM, quarter-wave plate Q, shear flow cell of the RSA-II, circular polarizer CP, and detector D. Signal analysis components: low-pass filter LPF and lock-in amplifier LI1. (b) Shear sandwich flow cell for measuring birefringence in the 1,3-plane.

broad temperature range (phase transitions: g 317 K (44 °C) n 390 K (117 °C) i, where g = glassy, n = nematic, and i = isotropic).[23] Synthesis of the monomers was performed in a three-step reaction. After a Williams etherification of p-HBA (*p*-hydroxybenzoic acid) with 6-chlorohexanol, an esterification with 4-methoxyphenol was performed using the DCCI (dicyclocarbodiimide) method.[24] Finally, the resulting functional alcohol is reacted with methacrylic acid. Deuterated methacrylic acid was synthesized by Dr. Naarmann at BASF. The monomer was purified using medium-pressure liquid chromatography (Kieselgel HD-SIL 60 Å, 16–24 μm, *tert*-butyl methyl ether/cyclohexane = 1:3).

The polymer was obtained by a free radical polymerization in 2-butanol with 0.5 mol % azobis(isobutyronitrile) (AIBN) as an initiator at 60 °C.[25] Molecular weight was determined by GPC using a standard of the same side-group liquid-crystalline polymer obtained from narrow molecular weight fractions with light scattering calibration.[26] Thermal characterization was done using DSC and DTA (Mettler DSC 30). Decomposition of the material started above 590 K (320 °C), indicating that the material was thermally stable under the conditions of the rheooptical experiments. This was confirmed by repeating thermal characterization of samples after the rheological experiments were completed. The sample used here has a bimodal molecular weight distribution, dominated by a high molecular weight fraction (76% vol) of $M_w \approx 3.2 \times 10^6$ g/mol ($M_w/M_n = 1.3$), with the remainder of lower molecular weight, $M_w \approx 2.5 \times 10^5$ g/mol ($M_w/M_n = 1.8$).

3.2. Apparatus. Optical and mechanical characterization was performed using a Rheometrics RSA-II dynamic mechanical testing system that has been modified to permit optical measurements. Dynamic birefringence was measured using a polarization-modulation scheme (optical train, Figure 2a). This rheooptical instrument has been described in detail elsewhere.[27] The principal features of this apparatus are the simultaneous observation of transient stress and birefringence over a wide frequency range at each temperature and over a broad range of operating temperatures. Oscillatory strain frequencies cover four decades (0.01–100 rad/s). Environmental control from −100 to +400 °C is achieved by circulating air or nitrogen through the environmental chamber. The uniformity and stability of the temperature are specified to be ±0.5 °C. Rheooptical measurements were performed using a "shear sandwich" geometry with the optical axis along the velocity gradient (Figure 2b). Custom shear sandwich fixtures were fabricated with the plates replaced by CaF_2 windows. The optical path in this case was twice the gap width, i.e., 1.30 mm.

The signals from the displacement and force transducers, the low-pass filter I_{dc}, and lock-in amplifier I_{1f} were recorded by a microcomputer at a rate that provided 128 points per cycle of the oscillatory strain at frequency ω. The strain, stress, and $R_{1f} \equiv I_{1f}/I_{dc}$ are calculated from these results. The data acquired over a number of cycles (typically 3–10) are then averaged. For a sample with zero dichroism and having a principal axis along the flow direction (0°), the ratio R_{1f} is related to the retardance μ of the sample by $R_{1f} = -2J_1(A) \sin \mu$, where $J_1(A)$ is the Bessel function of the first kind evaluated at the amplitude of the modulator[28] and $\mu = (2\pi d/\lambda)\Delta n'_{13}$, with d the optical path length, λ the wavelength of the incident light, and $\Delta n'_{13}$ the birefringence in the 1,3-plane (normal to the optical axis). From $R_{1f}(t)$, we calculate $\Delta n'_{13}(t)$. Next, the Fourier transforms of the time-domain signals are calculated. The second-harmonic component of $\Delta n'_{13}$ is used to determine the complex amplitude coefficient of the birefringence, $(\Delta n'_{13})^* = (\Delta n'_{13})' - i(\Delta n'_{13})''$.[30,31]

3.3. Methods. All of our oscillatory shear experiments were performed using the parallel-plate device shown in Figure 2, with a gap width of 0.65 mm and plates of 2-cm² area. Two types of oscillatory shear protocols were used: (1) frequency sweep experiments, where a small strain amplitude is used (<8%) to probe dynamic response as a function of frequency and (2) prolonged, large-amplitude (roughly 40%) oscillatory shear at a fixed frequency. Frequency sweep experiments were performed at temperatures from 75 to 130 °C. During the frequency sweep experiments in the isotropic phase, in which the sample is transparent, the shear stress and the birefringence in the 1,3-plane are simultaneously recorded.

For reference, the stress-optical behavior of SG-LCPs may be contrasted to that of amorphous, linear polymer melts in oscillatory shear. In amorphous polymer melts, the stress-optical rule holds over a wide range of flow conditions, so the complex amplitude of the 1,3-birefringence, $(\Delta n'_{13})^*$, equals $C\Psi_3^*$, where C is the stress-optic coefficient and Ψ_3^* is the complex amplitude of the third normal stress difference.[30,31] For linear, amorphous melts in small-amplitude oscillatory shear, $|\omega^2\Psi_3^*|$ is observed to equal $\kappa|G^*(\omega) - {}^1/_2G^*(2\omega)|$, where ω is the shear frequency and κ is the ratio of the third to the first normal stress differences ($\kappa = 0.74 \bullet 0.07$).[27] Therefore, we contrast the behavior of SG-LCPs in the isotropic phase to amorphous polymer melts by considering a stress-optic ratio based on 1,3-birefringence (SOR_{13}) defined as

$$SOR_{13} \equiv \frac{|\omega^2(\Delta n'_{13})^*|}{|G^*(\omega) - {}^1/_2G^*(2\omega)|}$$

If this coefficient is independent of frequency at a given temperature, it suggests that the stress-optic rule holds. In that case, the temperature dependence of SOR_{13} may be contrasted to amorphous polymer melts. If SOR_{13} depends on frequency, it suggests that the SG-LCP does not obey the stress-optic rule.

In the nematic state, frequency sweeps are used only to determine the effective dynamic moduli. Frequency sweeps are repeated before and after subjecting the nematic phase to prolonged large-amplitude shear. Results are presented for the effects of prolonged shearing at 110 °C for 800 cycles at a frequency of 1 rad/s and strain amplitude of 34%. To establish a reproducible initial condition for each large-amplitude shear experiment, the sample was held at a temperature well above T_{ni} (130 °C) for 30 min to eliminate any effects of the flow history. The sample was then cooled to 110 °C and allowed to reach thermal equilibrium (30 min). This procedure resulted in a reproducible initial state based on the transient shear stress observed during prolonged shear.

4. Results

The dynamic moduli G^* of the present SG-LCP were measured at 75, 80, 95, 110, 114, 115, 116, 117, 117.5, 118, 120, 125, and 130 °C. Results at only a few temperatures are shown in Figure 3a–c for clarity. Upon cooling through T_{ni}, the low-frequency dynamic moduli decrease abruptly. The particular way that time–temperature superposition fails at T_{ni} is best illustrated through a Cole–Cole plot (Figure 3c), which removes any ambiguity introduced by the procedure of time–temperature superposition. It

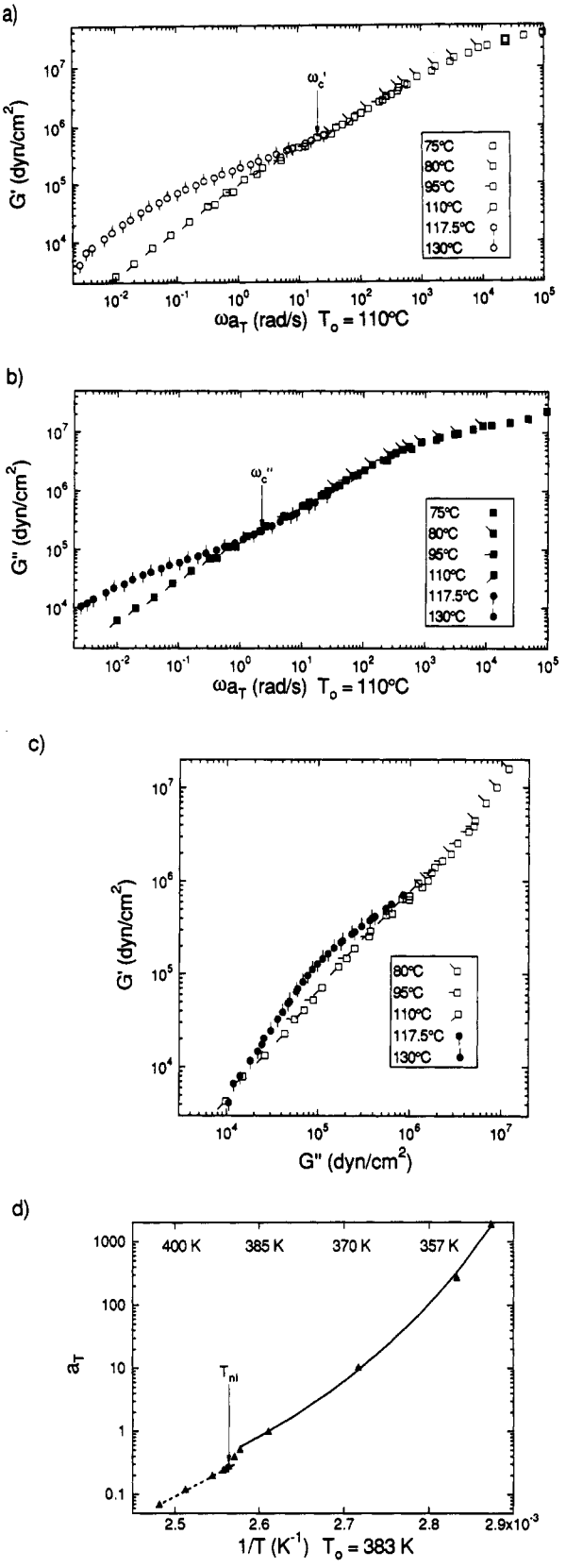

Figure 3. (a) Storage modulus master curve (G') of isotropic and unaligned nematic states. (b) Loss modulus master curve (G''). (c) Cole–Cole plot of the storage modulus versus the loss modulus. (d) Time–temperature shift factors (a_T) with respect to $T_0 = 110$ °C: points show the experimental values, dashed line shows Arrhenius behavior with $E_a = 32.6$ kcal/mol, and solid curve shows WLF behavior as described in the text.

shows that there are two distinct curves, one for the isotropic phase and one for the nematic phase; therefore, time–temperature superposition is appropriate within each phase. Above sufficiently high values of G' and G'', corresponding to frequencies above a critical frequency, the two curves appear to converge, suggesting that time–temperature superposition holds at high enough frequencies for both the isotropic and nematic phases. In Figure 3a,b it appears that the storage moduli of both phases superpose above $\omega_c' \approx 20$ rad/s and the loss moduli superpose above $\omega_c'' \approx 2$ rad/s.

The shift factors used for the master curves shown in Figure 3a,b are shown in Figure 3d. Like previous studies, we find that in the isotropic phase the shift factors show an Arrhenius temperature dependence. The apparent activation energy for flow is $E_a \approx 33$ kcal/mol. This is somewhat higher than the value reported by Zentel and Wu for a SG-LCP of the same chemical structure (E_a = 25 kcal/mol).[3] In the nematic phase we observed WLF behavior with $\log a_T = [-4.36(T - T_0)]/[82 + T - T_0]$ for a reference temperature $T_0 = 383$ K. Non-Arrhenius behavior of SG-LCP melt viscoelasticity in the nematic phase has not been reported previously. There appears to be a surprisingly large change in a_T from 117.5 to 115 °C.

Within the nematic state, the flow history can influence the flow response. Therefore, we refer to effective dynamic moduli observed in small-amplitude shear. Indeed, we have confirmed that the response at small strains is linear in the isotropic and nematic phase at all temperatures used by varying the strain over a five- to tenfold range (typically 0.5–8%). At the highest reduced frequencies the modulus is that characteristic of glassy behavior. Although there is the suggestion of a plateau region, it is not well defined. In monodisperse linear polymers, the plateau modulus can be obtained either by using the height of the plateau in the storage modulus or the value of the storage modulus at the minimum in the loss tangent.[32] Even though our sample is polydisperse, we use these methods to obtain a rough estimate of the plateau modulus. Based on this approximate value of $G_N°$, the entanglement molecular weight of this SG-LCP in the isotropic phase is roughly $M_e \approx 2 \times 10^5$ g/mol. Further experiments on narrow molecular weight fractions will be performed to determine M_e more precisely.

The effect of prolonged, large-amplitude oscillatory shear on the nematic phase is dramatic. Initially, after cooling from the transparent, isotropic state into the nematic state, the sample becomes opaque due to strong light scattering. As long as the sample is left at rest, the sample remains opaque, indicating that the defect texture that produces the scattering coarsens slowly, if at all. After performing frequency sweep experiments with small strain amplitude, there is also no evidence of coarsening. However, during the application of many cycles of large-amplitude oscillatory shear, the sample becomes translucent and eventually transparent.[33] In this state, when viewed through crossed polarizers oriented at ±45° with respect to the flow direction, the sample appears highly birefringent. Based both on the transparency and high birefringence, this is referred to as a flow-aligned state. After cessation of large-amplitude shear, small-amplitude dynamic viscoelastic measurements were performed at two different times: after 1 min and after 30 min. The results show that the effective dynamic moduli of the "aligned" sample are significantly reduced relative to the "unaligned" nematic as quenched from the isotropic state (Figure 4). In addition, the two sets of data are found to be in good agreement, which suggests that the reduction in the moduli may be permanent. The additional drop in G' and G'' due to flow alignment is confined to frequencies below ω_c' and

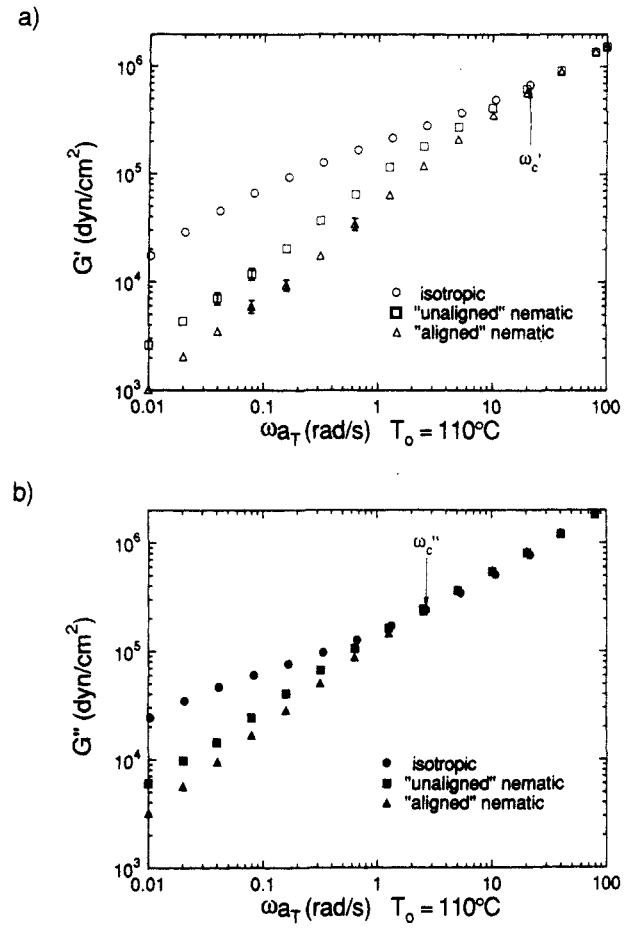

Figure 4. Effect of flow alignment on the dynamic moduli. Storage (a) and loss (b) moduli of the isotropic phase and of the nematic phase at 110 °C before and after large-amplitude shearing. The average of the values obtained in two separate series of experiments is shown by each symbol; where the difference between these values is greater than the symbol size, a vertical bar spans between them.

ω_c'', the critical frequencies evident in the effect of the isotropic–nematic transition on G^*.

In the isotropic state, the birefringence is monitored simultaneously with the stress during dynamic mechanical experiments. The results are presented in terms of the stress-optical ratio (SOR_{13}) defined in section 3. At sufficiently high temperatures, e.g., 130 °C, SOR_{13} is independent of frequency (Figure 5), supporting the applicability of the stress-optical rule, as is found for amorphous polymer melts. Indeed, the value of SOR_{13} at 130 °C has a magnitude ($\sim 8 \times 10^{-10}$ cm²/dyn) typical of many other amorphous polymer melts. As the temperature is reduced toward T_{ni}, SOR_{13} increases much more strongly than is observed for amorphous polymers, rising to $\sim 2 \times 10^{-9}$ cm²/dyn at 125 °C and $\sim 5 \times 10^{-9}$ cm²/dyn at 120 °C. Very close to T_{ni}, SOR_{13} depends on frequency; at the lowest frequencies we apply, SOR_{13} continues to increase as the system approaches the temperature at which it will spontaneously adopt nematic order. Even very near T_{ni}, SOR_{13} is independent of strain amplitude: at 117.5 °C, no effect of strain on SOR_{13} is found over a sixfold range of strain.

5. Discussion

The isotropic-to-nematic transition produces a significant drop in the storage and loss moduli of the present SG-LCP (Figure 3a,b). Analogous to what has been observed in block copolymers, this effect is manifested below critical frequencies (ω_c' and ω_c'').[21] Following the interpretation of similar behavior in block copolymers, this suggests that fast enough, i.e., sufficiently local, dynamics are not affected by the phase change, whereas sufficiently slow dynamics are sensitive to the change in microstructure.

The basic observation that the isotropic–nematic transition results in an abrupt change in the viscoelastic properties of this SG-LCP (see Figure 3) may be contrasted to the results of previous studies. Colby and co-workers[4] found no change in the magnitude or shape of the dynamic moduli of their SG-LCPs at T_{ni}. Direct comparison of our results with previous steady shear viscosity measurements is not possible.[3,4] Nevertheless, the observation that the viscosity of previously studied SG-LCPs does not change abruptly at T_{ni}[2,3] is qualitatively different from the sudden drop in viscosity our results would suggest: the observed drop in $|G^*|$ of the present SG-LCP at T_{ni} tends to indicate that the zero-shear viscosity η_0 decreases abruptly, since η_0 equals the integral of the relaxation modulus. Such a drop in η_0 for this SG-LCP must be confirmed by extending measurements to the terminal regime.

The reason that a discontinuous change in the viscoelastic properties is observed in the present SG-LCP but not in previous samples is not yet known. It is unlikely to be the particular monomeric structure, given that a sample having the same chemical structure was among those studied by Zentel and Wu.[3] One of the distinctive features of the present sample is that its molecular weight (main GPC peak at 3.6×10^6 g/mol) is much higher than the materials used in previous studies (1.6×10^4 to 1.3×10^5 g/mol). Future work will examine the molecular weight dependence of the discontinuous change in the dynamic moduli at T_{ni}, which may reveal the origin of the discrepancy between our findings and those of other researchers.

Another distinction between our rheological results and earlier studies is in the temperature dependence of the time–temperature shift factor a_T (Figure 3d). In the nematic phase we find WLF behavior, expected for a polymer melt over a similar range of temperatures above the glass transition temperature. All previous studies have reported Arrhenius behavior, even at temperatures as close to T_g as those in our experiments. In the isotropic phase we do observe Arrhenius behavior with an activation energy comparable to that found in previous studies.

Entanglement behavior of SG-LCPs has not been characterized. Previous samples have been both polydisperse and, apparently, too short to be entangled. The present sample is also polydisperse, which probably explains the lack of a well-defined plateau in the storage modulus; however, the molecular weight is high enough to permit estimation of the plateau modulus. It is roughly an order of magnitude smaller than that of common amorphous polymers, suggesting a correspondingly larger entanglement molecular weight. The estimated value of $M_e \approx 2 \times 10^5$ g/mol is reasonable in light of the effect of side groups on the entanglement molecular weight of methacrylate backbone polymers.[32] Future characterization of relatively narrow molecular weight fractions of this SG-LCP will enable precise determination of the plateau modulus of the isotropic and nematic phases.

Pretransitional phenomena arising from orientation fluctuations in the isotropic phase near T_{ni} in SG-LCPs have previously been sought in the magnetic and electric susceptibility of these materials. In high molecular weight SG-LCPs (degree of polymerization above 100), little evidence of pretransitional effects has been found.[17] This

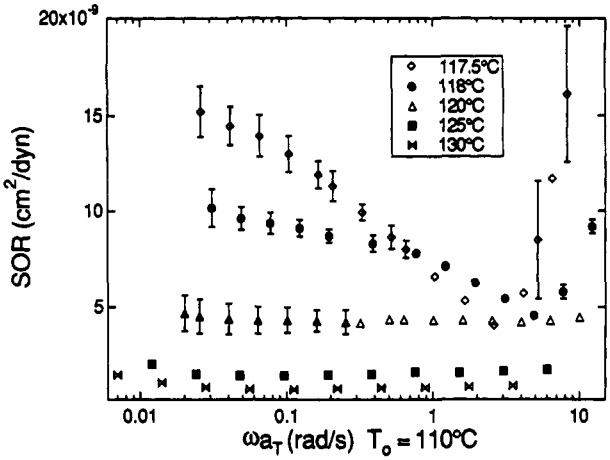

Figure 5. Stress-optic ratio in the isotropic phase near the isotropic–nematic transition. The results of two sets of measurements are shown. The average of the two values at each temperature and frequency is shown by a symbol; where the difference between the individual values is greater than the symbol size, a vertical bar spans between them.

has been attributed to the high viscosity of the materials. Stress-optical measurements on SG-LCP networks have proved successful in detecting the dramatic increase in the ratio of the birefringence to the stress that is expected as $T \rightarrow T_{ni}$.[18] Here we present the first results of flow birefringence measurements on SG-LCP melts (Figure 5). These show that the stress-optic ratio in the isotropic phase rises dramatically as the material is cooled toward the transition.

Further, our results suggest that very near T_{ni} the stress-optic rule fails: SOR_{13} becomes shear frequency dependent. However, we find that even in this regime, SOR_{13} remains independent of strain amplitude over a sixfold range of strain. A similar phenomenon has been observed in concentrated solutions of rigid-rod polymers near the isotropic–nematic transition, where the stress-optic ratio diverges and becomes shear rate dependent.[20] In the case of rigid rods, the shear rate dependence could be attributed to polydispersity in the sample. This interpretation cannot be applied to SG-LCPs, as the tendency of the mesogens to align locally controls the pretransitional behavior, and the mesogens are all identical. It may be significant that when SOR_{13} becomes frequency dependent, it has a minimum in the vicinity of ω_c' and ω_c''. Concerning the behavior for $\omega \lesssim \omega_c$, the decrease of SOR_{13} with increasing frequency might be understood in terms of probing progressively more local dynamics until the molecular responses to the deformation are on a small enough scale that they are no longer sensitive to long-range order in the surroundings. However, this explanation leads one to expect that SOR_{13} would become independent of frequency for $\omega > \omega_c$, failing to explain the increase in SOR_{13} with ω in the high-frequency regime.

In the nematic phase, we report evidence that oscillatory shear induces a preferred macroscopic alignment in this SG-LCP. This behavior is reminiscent of the flow-induced alignment of block copolymers in cylindrical or lamellar phases. Analogous to block copolymers, the effective dynamic moduli decrease as a result of flow alignment. This is consistent with the idea that one of the mechanisms of flow alignment involves the tendency of fluids that possess intrinsically anisotropic viscoelastic properties to adopt an orientation that reduces their resistance to flow.[9] In addition, like block copolymers, the critical frequencies below which the dynamic moduli are sensitive to microstructural alignment coincide with ω_c' and ω_c'' below which G' and G'' are affected by the phase transition. Again, this is consistent with the view that sufficiently rapid dynamics are insensitive to the long-range order in these fluids.

The observation that this high molecular weight, nematic, side-group liquid-crystal shows some of the distinctive viscoelastic features observed in ordered block copolymers suggests that these responses may arise from those features the two systems have in common. Most notably, both fluids possess intrinsically anisotropic local structure and appear to have orientation-dependent viscoelastic properties. In addition, both systems possess a broad spectrum of relaxation processes. Evidently, the slowest relaxation dynamics in each case are sensitive to the changes in fluid structure associated with ordering transitions and flow alignment. Perhaps these general features underlie the shared rheological characteristics of these two qualitatively different types of polymer melts, in spite of their very different molecular architectures and fluid microstructures.

6. Conclusion

This study shows that side-group liquid-crystalline polymers *can* undergo flow alignment, contrary to the conclusions of previous studies. The viscoelastic behavior of the present SG-LCP shows numerous analogies to block-copolymer (BCP) melts: (i) there is a discontinuous jump in the dynamic moduli at the isotropic–nematic transition, like that observed at the ordering transition of BCPs, (ii) there exist critical frequencies below which the viscoelastic properties are sensitive to the isotropic–nematic phase transition and to flow alignment of the nematic, (iii) macroscopic alignment of the nematic can be induced by shearing, and (iv) flow-induced alignment is accompanied by a decrease in the dynamic moduli. Our rheooptical results show that SG-LCPs exhibit pretransitional effects in their stress-optical behavior, analogous to those observed in lyotropic rigid-rod LCPs.

These results raise questions regarding the origin of the discrepancy between our findings and previous studies of SG-LCP melts and the mechanism of flow alignment in SG-LCPs. To understand the distinctions between the behavior of the present SG-LCP ($M_w > 1 \times 10^6$ g/mol) and samples studied previously ($M_w < 2 \times 10^5$ g/mol), we will first examine the effect of molecular weight. To clarify the nature of the flow alignment process and the degree and direction of molecular orientation it produces, further experiments are required. The evolution of the dynamic moduli and the transmittance during large-amplitude shear are described in a separate publication.[33] We plan to use simultaneous measurements of strain, stress, and infrared dichroism to correlate the responses of the side groups and the backbone with the macroscopic changes that occur. Light scattering and microscopy will be used to characterize the microstructure in samples quenched at intermediate stages of flow alignment. Together these will provide a detailed picture of the microstructural response of SG-LCPs during dynamic shear.

Acknowledgment. We gratefully acknowledge the support of the National Science Foundation Presidential Young Investigator Award (J.A.K.), the Gates Grubstake Fund, and the NATO-Travel Grant Program (CRG 901037). We thank Ute Pawelzik at the Max-Planck-Institut für Polymerforschung for synthesizing the polymers for this research.

References and Notes

(1) McArdle, C. B., Ed. *Side Chain Liquid Crystal Polymers*; Blackie: Glasgow; in U.S.A., Chapman and Hall: New York, 1989.
(2) Fabre, P.; Veyssie, M. *Mol. Cryst. Liq. Cryst. Lett.* **1987**, *4*, 99.
(3) Zentel, R.; Wu, J. *Makromol. Chem.* **1986**, *187*, 1727.
(4) Colby, R. H.; Gillmore, J. R.; Galli, G.; Laus, M.; Ober, C. K.; Hall, E. Linear viscoelasticity of side-chain liquid-crystal polymers, submitted to *Mol. Cryst. Liq. Cryst.* (1992).
(5) Porter, R. S.; Johnson, J. F. In *Rheology*; Eirich, F. R., Ed.; Academic Press: New York, 1967; Vol. 4, Chapter 5.
(6) Wissbrun, K. F.; Griffin, A. C. *J. Polym. Sci., Polym. Phys. Ed.* **1982**, *20*, 1835.
(7) Baird, D. G. In *Liquid Crystalline Order in Polymers*; Blumstein, A., Ed.; Academic Press: New York, 1978.
(8) Papkov, S. P.; Kulichikhin, V. G.; Kalmykova, V. D.; Malkin, A. Y. *J. Polym. Sci., Polym. Phys. Ed.* **1974**, *12*, 1753.
(9) Hadziioannou, G.; Mathis, A.; Skoulious, A. *Colloid Polym. Sci.* **1979**, *257*, 15, 22, 136, 344.
(10) Doi, M.; Edwards, S. F. *The Theory of Polymer Dynamics*; Clarendon Press: Oxford, 1988.
(11) Gleim, W.; Finkelmann, H. *Makromol. Chem.* **1987**, *188*, 1489.
(12) Pakula, T.; Zentel, R. *Makromol. Chem.* **1991**, *192*, 2401.
(13) de Gennes, P.-G. *Mol. Cryst. Liq. Cryst.* **1971**, *12*, 193.
(14) de Gennes, P.-G. *The Physics of Liquid Crystals*; Clarendon Press: Oxford, 1974.
(15) Eich, M.; Ullrich, K.; Wendorff, J. H. *Prog. Colloid Polym. Sci.* **1984**, *69*, 94.
(16) Stinson, T. W.; Lister, J. D. *Phys. Rev. Lett.* **1970**, *25*, 503.
(17) Fuhrmann, K.; Dries, T.; Fischer, E. W.; Ballauff, M. *J. Polym. Sci., Polym. Phys. Ed.* **1992**, *30*, 1199.
(18) Schätzle, J.; Kaufhold, W.; Finkelmann, H. *Makromol. Chem.* **1989**, *190*, 3209.
(19) Hammerschmidt, K.; Finkelmann, H. *Makromol. Chem.* **1989**, *190*, 1089.
(20) Mead, D. W.; Larson, R. G. *Macromolecules* **1990**, *23*, 2524.
(21) Rosedale, J.; Bates, F. S. *Macromolecules* **1990**, *23*, 2329.
(22) Portugall, M.; Ringsdorf, H.; Zentel, R. *Makromol. Chem.* **1982**, *183*, 2311.
(23) We found no evidence of a smectic phase in results of DSC, polarization microscopy, or deuteron NMR spectroscopy. However, annealed SG-LCPs of the same structure but lower molecular weight and narrow molecular weight distribution have been shown to possess a weak smectic (SmA1) phase as evidenced in SANS measurements with $T_{sn} \approx 73$ °C. See: Noirez, L.; Keller, P.; Cotton, J. P. *J. Phys. I Fr.* **1992**, *2*, 915 and references therein. Even if such a phase is present in this sample, it would not affect the interpretations of our results, because the flow alignment experiments are performed close to T_{ni} and well above 73 °C.
(24) Neises, B.; Steglich, W. *Angew. Chem.* **1978**, *90*, 556.
(25) Dames, B. Ph.D. Thesis, Mainz, 1990.
(26) Ohm, H. Ph.D. Thesis, Mainz, 1985.
(27) Kannan, R. M.; Kornfield, J. A. *Rheol. Acta* **1992**, *31*, 535.
(28) Johnson, S. J.; Frattini, P. L.; Fuller, G. G. *J. Colloid Interface Sci.* **1985**, *104*, 440.
(29) Janeschitz-Kriegl, H. *Polymer Melt Rheology and Flow Birefringence*; Springer: New York, 1983.
(30) Kornfield, J. A.; Fuller, G. G.; Pearson, D. S. *Rheol. Acta* **1990**, *29*, 105.
(31) Kornfield, J. A.; Fuller, G. G.; Pearson, D. S. *Macromolecules* **1991**, *24*, 5429.
(32) Wu, S. *J. Polym. Sci., Polym. Phys. Ed.* **1989**, *27*, 723.
(33) Kannan, R. M.; Kornfield, J. A.; Schwenk, N.; Boeffel, C. Shear-Induced Orientation of Side-Group Liquid-Crystalline Polymers., to be submitted to *Adv. Mater.*
(34) It was not possible to capture the terminal regime in the frequency range of our instrument (10^{-2}–10^{2} rad/s) at the temperatures employed. For the isotropic phase future experiments may overcome this limitation by using higher temperatures; for the nematic phase, we are limited to $T < T_{ni}$. In addition, previous studies[2,3] do not indicate whether or not the limiting value of the zero-shear viscosity η_0 was reached.